Supramolecular Chemistry

Supramolecular Chirality of Hydrogen-Bonded Rosette Assemblies

Socorro Vázquez-Campos[a]; Mercedes Crego-Calama[a]; David N. Reinhoudt[a]

[a] Laboratory of Supramolecular Chemistry and Technology, MESA+ Institute for Nanotechnology and Faculty of Science and Technology, University of Twente, Enschede, AE, The Netherlands

PLEASE SCROLL DOWN FOR ARTICLE

Supramolecular Chirality of Hydrogen-Bonded Rosette Assemblies

SOCORRO VÁZQUEZ-CAMPOS, MERCEDES CREGO-CALAMA* and DAVID N. REINHOUDT

Laboratory of Supramolecular Chemistry and Technology, MESA$^+$ Institute for Nanotechnology and Faculty of Science and Technology, University of Twente, P.O. Box 217 7500, AE, Enschede, The Netherlands

The control of chirality in synthetic self-assembled systems remains challenging because of their lower stability and their higher susceptibility to racemization when compared to covalent systems. In this review the supramolecular chirality of noncovalent hydrogen-bonded assemblies formed by multiple cooperative hydrogenbonds between calix[4]arene dimelamines and cyanurates or barbiturates derivatives (rosette assemblies) are described. It is shown that the amplification of chirality (a high enantiomeric or diastereomeric excess induced by a small initial amount of chiral bias) of double and tetrarosette assemblies is influenced by bulky substitution on their components and electronic properties of the substituents as well as their proximity to the rosette core. In the absence of chiral centers in their components, the assemblies form as a racemic mixture of both enantiomers (*P* and *M*). The synthesis of enantiomerically pure rosette assemblies is conducted via induction of chirality using chiral barbiturates, followed by substitution of the chiral components for achiral cyanurates ("chiral memory" concept). The addition of an external auxiliary to a racemic mixture of *P* and *M* assemblies leading to the formation of one of the two possible diastereomeric assemblies is also described. Moreover, chiral resolution of self-assembled nanostructures on highly oriented pyrolytic graphite (HOPG) surfaces is also discussed.

Keywords: Supramolecular chirality; Noncovalent synthesis; Amplification of chirality; Diastereomeric synthesis; Enantiomeric synthesis; Hydrogen-bonds

INTRODUCTION

The three dimensional arrangement of atoms in molecules defines the molecular stereochemistry. In the case of supramolecular structures, the supramolecular stereochemistry [1] comes from the spatial arrangement of their molecular components which are held together by weak interactions. Supramolecular chirality plays an important role in life; [2] nearly all biological polymers are optically pure meaning that all their components have the same handedness. All amino-acids in proteins are "left handed" while all sugars in DNA, RNA and in the metabolic pathway are "right handed". Therefore, the control of supramolecular chirality has become an important issue to understand biological processes such as protein folding or the expression and transfer of genetic information. Supramolecular chirality results from both the properties of the components and the way in which they associate. Therefore, the chirality of the system at the supramolecular level can be formed by the association of chiral components [3,4] as well as by a dissymmetric interaction of achiral components [5–17]. Self-assembly of supramolecular structures occurs via non-covalent interactions such as hydrogen bonding, coordination, aggregation, and electrostatic interactions. Especially hydrogen bonding interactions [18,19] contribute in the selectivity of processes such as molecular recognition, self-assembly, biomimicking as well as supramolecular chirality [20–24].

Clear examples of stereochemical selectivity in noncovalent synthesis can be observed in the rosette assemblies. These are obtained by the combination of building blocks with complementary hydrogen bonding motifs (three melamines and three iso-cyanuric acid (CYA) or barbituric acid (BAR)) (Fig. 1) [25–27]. This rosette motif forms large and well-defined hydrogen-bonded structures. The formation of double rosette assemblies is induced by mixing
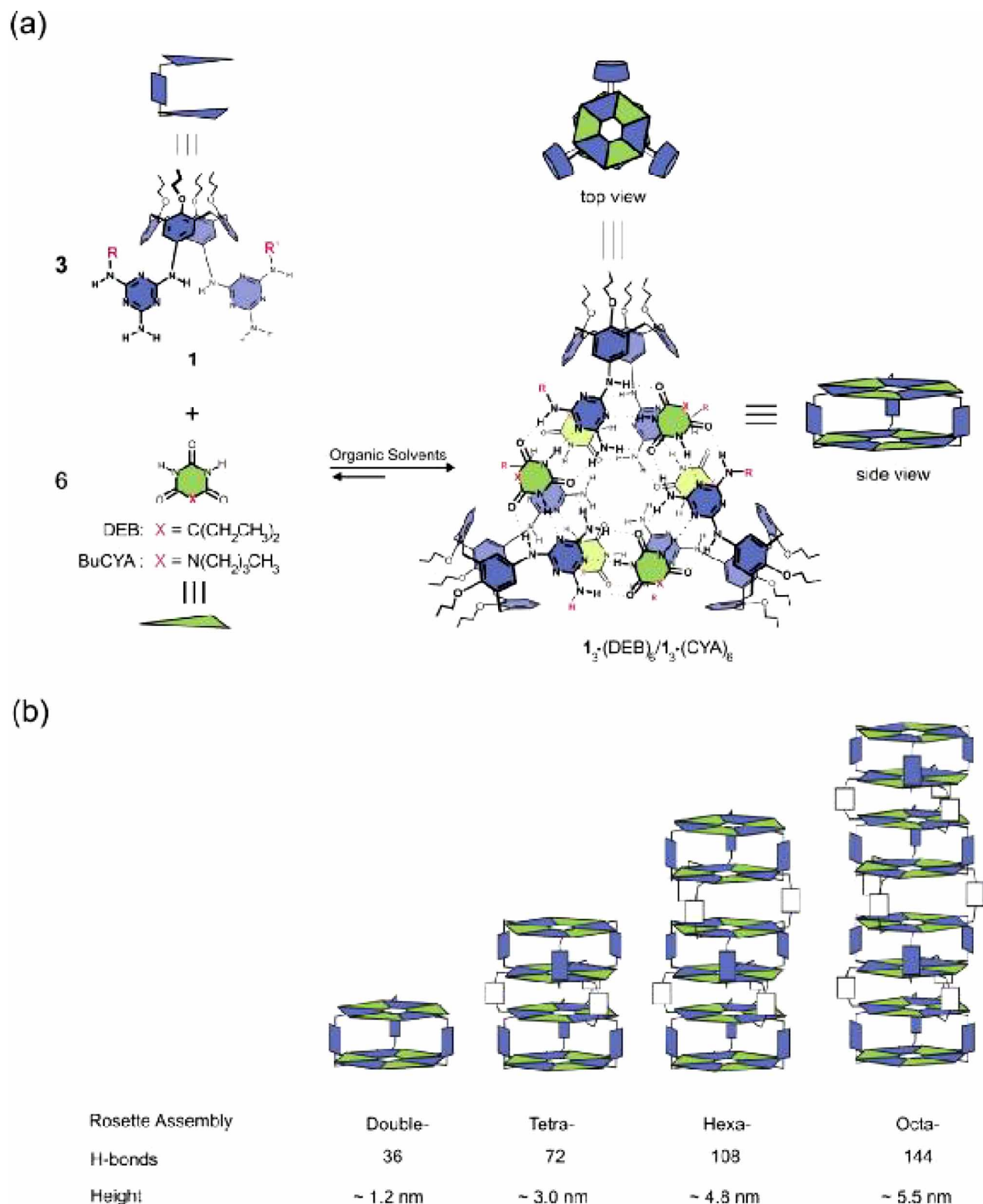
FIGURE 1   (a) Formation of double rosette assembly $1_3 \cdot (DEB)/1_3 \cdot (BuCYA)_6$ from three calix[4]arene dimelamines 1 and six 5,5-diethylbarbiturate (DEB) or n-butyl cyanurate (BuCYA) building blocks. (b) Schematic representation of double, tetra, hexa and octarosettes. Each floor represents one rosette motif.

calix[4]arene derivatives, diametrically substituted with two melamine units at the upper rim, with two equivalents of BAR or CYA (Fig. 1) [28]. Extended tetra-, hexa- and octarosettes are obtained when calix[4]arene dimelamine units are covalently linked [29–31]. The rapid increase of number of hydrogen bonds (double rosette = 36, tetrarosette = 72, hexarosette = 108 and octarosette = 142) in these

extended assemblies renders a high thermodynamic stability (Fig. 1).

In this review, the control of the chirality of hydrogen-bonded assemblies based on rosette motif at three different levels is described. Amplification of chirality ("sergeant and soldiers" principle), which takes place when the achiral building blocks of the assemblies follow the helicity induced by the chiral components even when the chiral molecules are present in very small amounts. Enantioselective noncovalent synthesis (memory of supramolecular chirality) is also described where the use of a chiral building block interacts stereoselectively to give preferentially one of the two possible diastereomeric forms (*P* or *M*-helix). After the replacement of the chiral building block by an achiral analog the induced chirality is preserved leading to the synthesis of enantiomerically enriched double rosette assemblies. Furthermore, diastereomeric and enantiomeric noncovalent synthesis of double rosettes can be achieved by the introduction of a chiral guest; therefore inducing the formation of one specific helicity of the rosette assemblies. The studies on enantioselectivity and amplification of chirality in extended systems, tetrarosette assemblies, are also presented. Moreover, the induction of chirality observed for these hydrogen-bonded rosette assemblies on highly oriented pyrolytic graphite (HOPG) surfaces is also reviewed.

ROSETTE ASSEMBLIES: FORMATION AND CHARACTERIZATION

Double rosette assemblies $1_3 \cdot (DEB)/1_3 \cdot (CYA)_6$ are held together by a total of 36 hydrogen bonds. The assemblies are formed spontaneously by mixing calix[4]arene dimelamines **1** with 2 equivalents of either barbituric acid (BAR) or cyanuric acid (CYA) derivatives in apolar solvents such as chloroform, benzene or toluene (Fig. 1) [28,32]. Three conformational isomers of double rosette assemblies can be formed D_3-, C_{3h}- and C_s-isomers (Fig. 2) [33,34]. The assemblies with D_3-symmetry, which is the predominant isomer, are chiral due to the staggered (antiparallel) orientation of the two melamine on each calix[4]arene unit, leading to a twist of the two different rosette planes, which can either adopt a clockwise ((P)-isomer) or counterclockwise ((M)-isomer) conformation. In both C_{3h}- and C_s-isomers, the two melamines on each calix[4]arene unit adopt an eclipse (parallel) conformation and are therefore achiral. The difference between the C_{3h}- and C_s-isomers is the 180° rotation of one of the calix[4]arene dimelamines.

Double rosette assemblies can conveniently be characterized by ^{1}H-NMR spectroscopy in solution [32]. Upon formation of the assembly the diagnostic signals for the BAR/CYA hydrogen-bonded imide NH protons are present in the region between
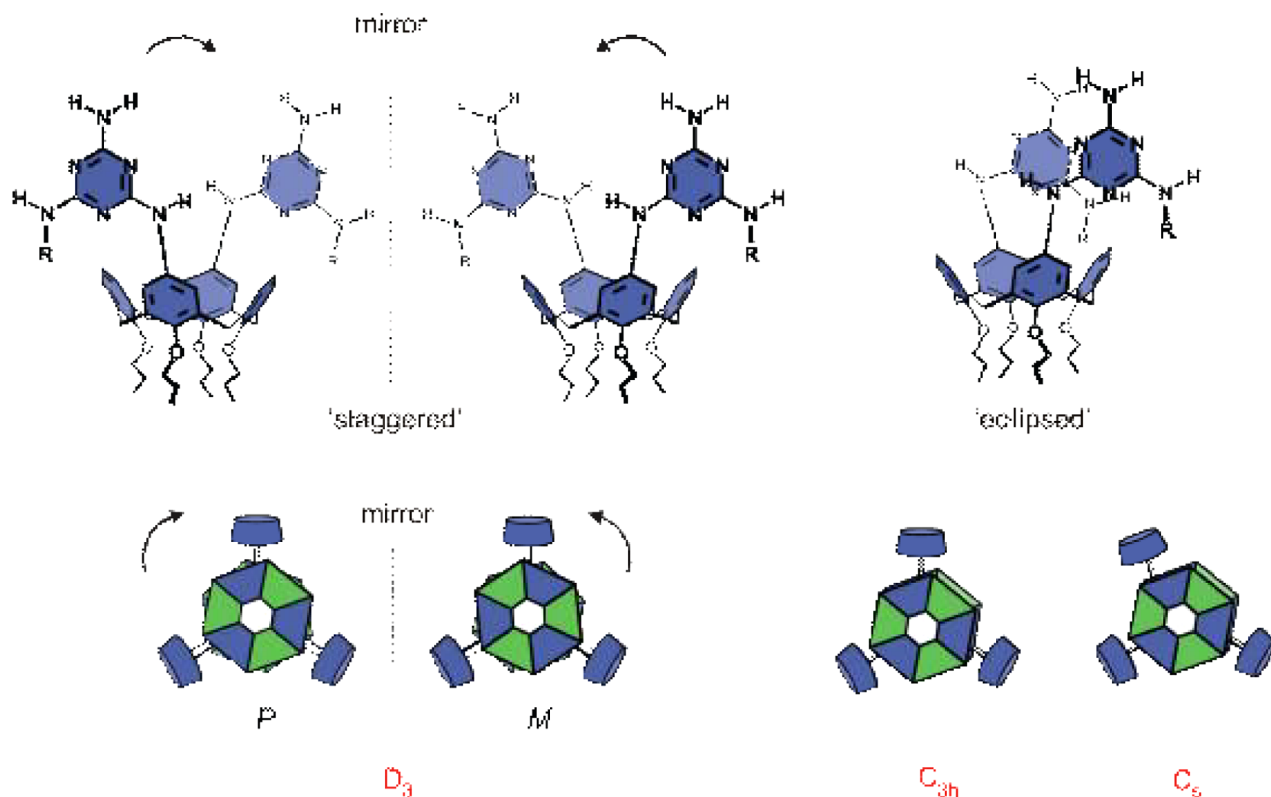

FIGURE 2   Schematic representation of the three isomeric forms for double rosette assemblies: Staggered (D_3), symmetrical eclipsed (C_{3h}), and unsymmetrical eclipsed (C_s).

13 ppm and 16 ppm. The number of signals that is observed indicates the symmetry type of rosette and the symmetry of the assembly. For example, for the D_3 and the C_{3h} symmetry isomers of the double rosette only two different hydrogen-bonded imide NH protons can be distinguished and therefore showing two different signals in the ^{1}H NMR spectrum. However, for the C_s isomer six signals are observed due to the magnetic differences between the six-hydrogen-bonded imide NH protons [35]. For assemblies formed with some bulky CYA derivatives all possible isomers were formed [33], while with BAR derivatives preferentially the D_3 isomers were obtained.

Hydrogen-bonded tetrarosette assemblies are extended rosettes formed by the association of three calix[4]arene tetramelamines (two calix[4]arene dimelamines covalently connected through two urea moieties) and 12 barbituric acid or cyanuric acid derivatives (Scheme 1). The building blocks are held together via 72 cooperative hydrogen bonds leading to the formation of a fully assembled tetrarosette structure $2_3 \cdot (DEB)_{12}$.

Rosette assemblies in general are formed as a racemic mixture of both (*M*)- and (*P*)-enantiomers when the components do not contain chiral centers [9,28,32,36]. However, complete induction of supramolecular chirality can be obtained for rosette assemblies when one of the building blocks is chiral. The (*M*)-diastereomer is formed when *R,R* dimelamines assemble with BAR or CYA, while the assembly of *S,S* dimelamines with BAR or CYA gives only the (*P*)-diastereomer (Scheme 2). This property makes it possible to study the rosette formation using circular dichroism (CD) spectroscopy [37]. It has been observed that, for example, double rosette assemblies exhibit a very strong induced CD signal ($|\Delta\varepsilon_{max}| \sim 100 \, l \, mol.^{-1} cm.^{-1}$), while the individual chiral components are hardly CD active ($|\Delta\varepsilon_{max}| < 8.1 \, l \, mol.^{-1} cm.^{-1}$). Therefore, the observation of CD signal is a direct result of the assembly formation. The CD curves of the (*M*)- and (*P*)-assemblies are perfect mirror images, reflecting their enantiomeric relationship (Scheme 2).

Another characterization technique is the MALDI-TOF mass spectrometry using the Ag^+ labeling approach [34]. This technique is extremely mild and provides a nondestructive method to generate positively charged assemblies by coordination of Ag^+ to two cooperative π-donors, cyano or other functionalities. Finally, X-ray crystallography provides unequivocal evidence that the assembly $1_3 \cdot (DEB)_6$ exists as the D_3-isomer (Fig. 3). Furthermore, it shows that the calix[4]arene units are fixed in a *pinched cone* conformation, which is the only conformation that allows simultaneous participation
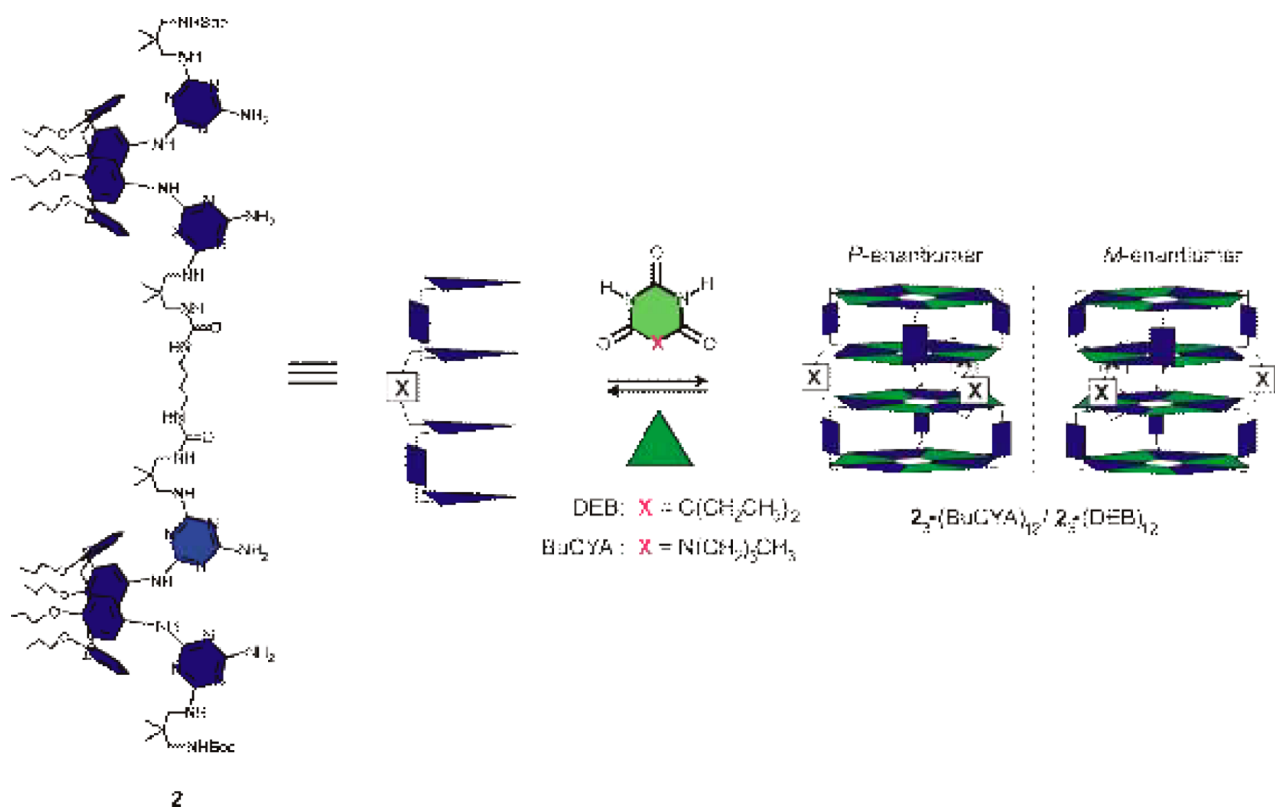
SCHEME 1 Formation of tetrarosette assembly $2_3 \cdot (DEB)_{12} / 2_3 \cdot (BuCYA)_{12}$ from three tetramelamines **2** and twelve 5,5-dyethylbarbituric acid (DEB) or butyl cyanuric acid (BuCYA) molecules.
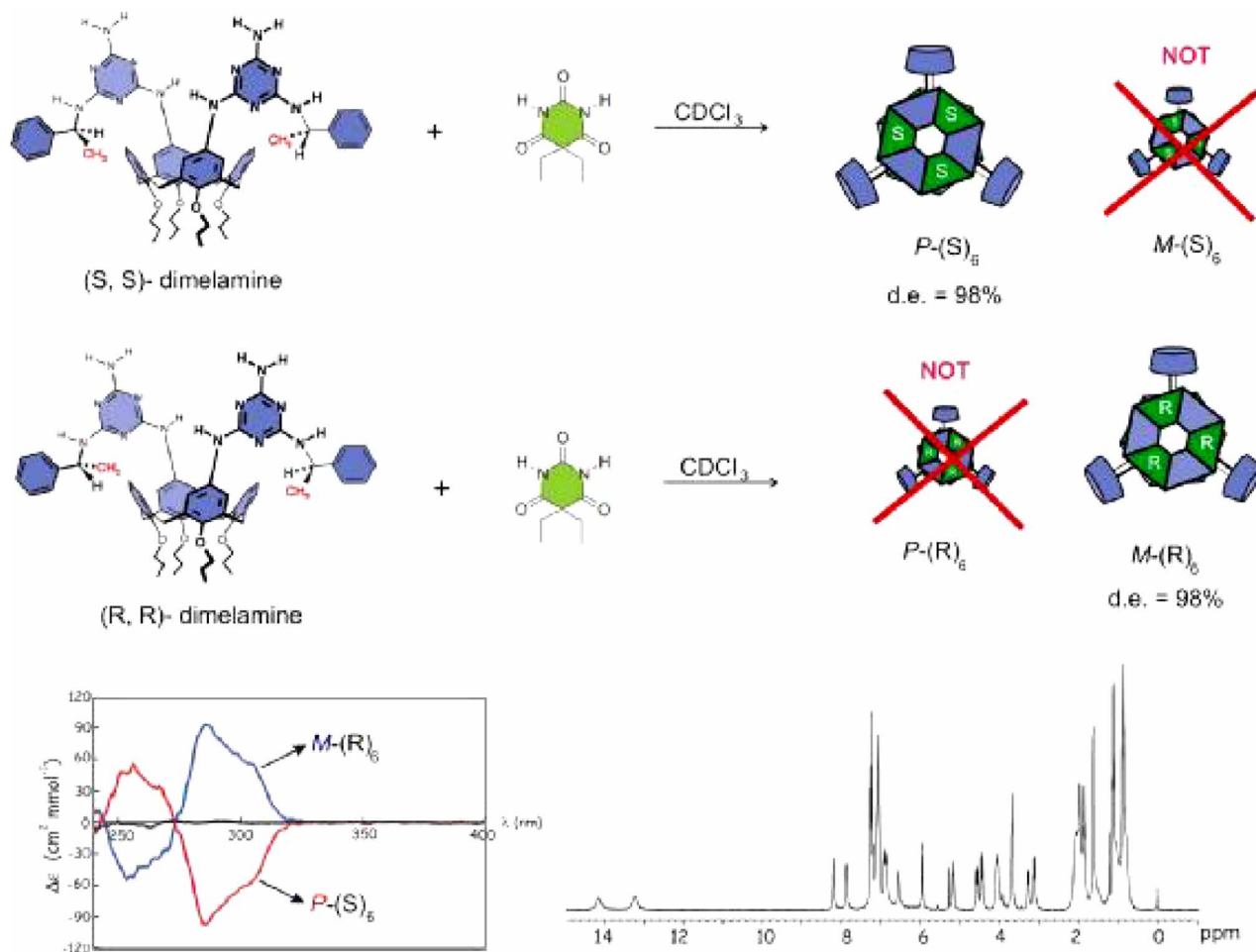
SCHEME 2 Representation of the process of induction of supramolecular chirality in double rosette assemblies. Examples of their characterization by CD and by ^{1}H-NMR are also shown.

of the calix[4]arene units in both the upper and the lower rosette motif. The two rosette motifs are stacked on top of each other with an interatomic separation of 3.5 Å at the edges to 3.2 Å in the centre of the rosette [32]. The assembly dimensions are 1.2 nm height and ~3 nm width.

THE CONTROL OF THE SUPRAMOLECULAR CHIRALITY IN HYDROGEN-BONDED ROSETTE ASSEMBLIES

Supramolecular assemblies exhibit well-defined topologies, determined by the arrangement and
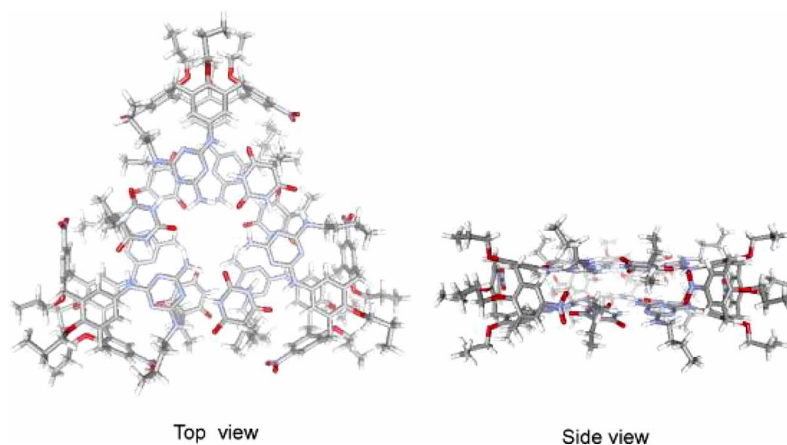

Top view   Side view

FIGURE 3 Top and side view of the X-ray structure of assembly $\mathbf{1}_3 \cdot (DEB)_6$.

connectivity of their molecular components. Therefore, supramolecular chirality involves the non-symmetrical arrangement of molecular components in noncovalent assemblies. The general method for controlling supramolecular chirality is the introduction of chiral substituents into the components, resulting in a mixture of two diastereomers. On the other hand, the achiral components can be assembled in such a way that the assembly has no elements of symmetry. Therefore, supramolecular structures can be prepared in a diastereomeric or enantiomeric form via noncovalent synthesis.

### Diastereoselective Noncovalent Synthesis

The general method to control the supramolecular chirality is via the introduction of chiral centers in the components of the assembly. The noncovalent diastereomeric synthesis of double rosette assemblies was achieved in two different ways. First, by the introduction of chiral centers in one of their components (calix[4]arene dimelamine or barbituric/cyanuric acid derivatives) (Scheme 3).

As a consequence six chiral centers are obtained in close proximity to the core of the assembly [9]. The presence of chiral centers in the dimelamines of the calix[4]arene or in the cyanurate derivatives induces quantitatively the formation of one handedness (*P* or *M*) of the hydrogen-bonded double rosette assemblies. Chiral barbiturates were also studied obtaining a smaller inducing effect in contrast to chiral dimelamines or cyanurates. From these studies it has been concluded that the chiral induction is related to the distance between the chiral centers and the core of the assembly. All diasteromerically pure assemblies presented very high CD activities compare to the correspondent free components. This method gives assemblies with a diastereomeric excess (d.e.) of 96%. Important information about the symmetry of the assembly is also obtained by ^{1}H-NMR spectroscopy [38].

The second method to achieve the diastereoselective synthesis of the assemblies is via complexation of chiral acids or diacids with a racemic mixture of amino-substituted double rosette assemblies [39,40]. Amino functionalities positioned on a noncovalent
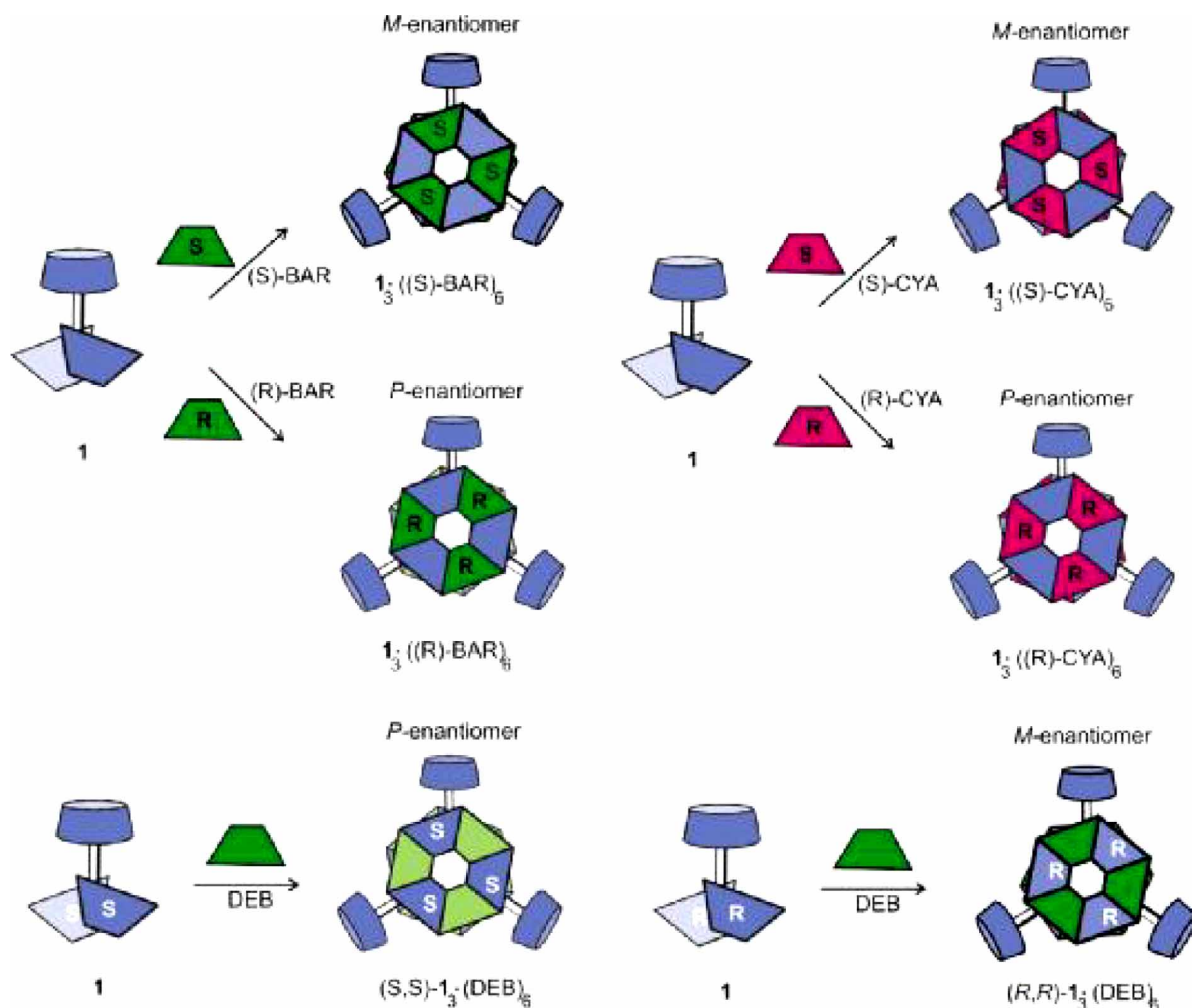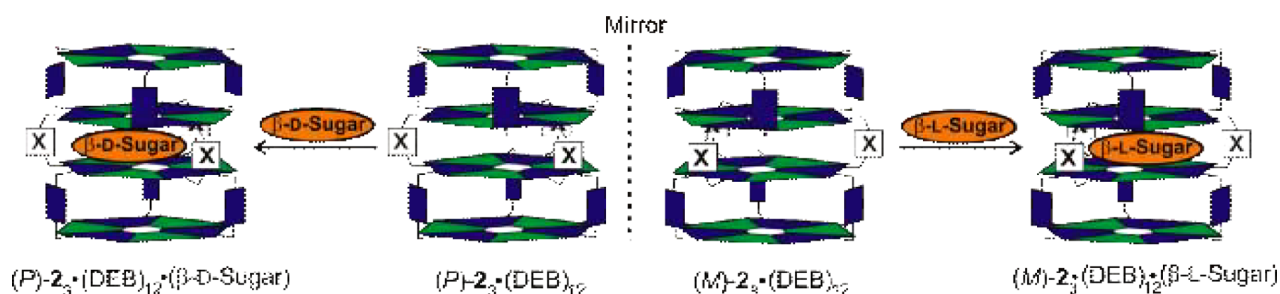

SCHEME 3   Schematic representation of the diastereomeric noncovalent synthesis of double rosette assemblies by introducing chirality in the dimelamines of the calix[4]arene (bottom) and in the barbiturates or cyanurates (top).
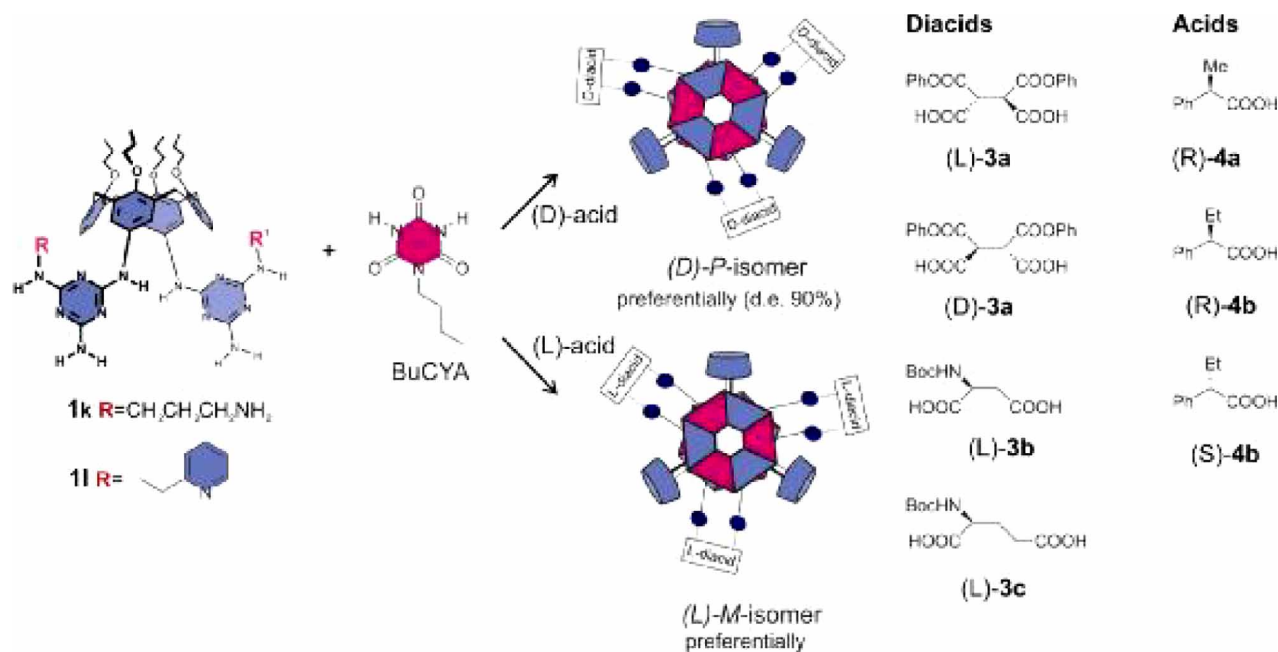
SCHEME 4   Illustration of induction of chirality by external chiral acids and diacids and molecular structures of the different acids and diacids studied.

rosette platform stereospecifically recognize carboxylic acids with detailed structural selectivities, both with respect to the substrate and the platform. The recognition takes place first by acid–base interactions [13,41–43]. The double rosette hydrogen-bonded assembly is used as a platform to organize the six amino functionalities at the periphery acting as binding sites for guest complexation (Scheme 4). The interaction between host and guest becomes clear from the shifts of the signals in the ^{1}H-NMR spectrum. The chiral acids present a clear selectivity in binding towards one of the enantiomers (M or P) of the double rosette assembly forming the corresponding diastereomeric complexes. Therefore, the enantiomer that is bound most strongly is amplified in the mixture causing the CD spectrum of the assembly to show Cotton effects in the presence of these chiral acids [40]. With this methodology we obtained assemblies which have a d.e. of ∼90%.

Moreover, supramolecular chirality can be observed with tetrarosette assemblies upon saccharide complexation [44]. Recognition of n-octyl β-D-glucopyranoside (β-D-Sugar, Scheme 5) by the tetrarosette (P)-2_3·(DEB)$_{12}$ is reflected by the shifts and splitting of the proton signals on the second and third rosette floors in the ^{1}H-NMR spectrum, whereas the corresponding signals of the first and fourth floor show no splitting. Addition of the chiral saccharide leads to an increase in the intensities of the proton signals indicating that only one of the two enantiomers of the racemic mixture recognizes the chiral guest. The stereoselective recognition process results in the formation of one diastereomeric system. Moreover, CD data gives also evidence that there is a preferential formation of the enantiomer that binds more strongly to the chiral saccharide guest, being CD active while the racemic mixture was CD silent. In conclusion, the chirality of the

SCHEME 5   Schematic representation of the process of induction of supramolecular chirality in tetrarosette assemblies $(P)/(M)$-2_3·(DEB)$_{12}$ by recognition of chiral saccharides (β-D-Sugar and β-L-Sugar).
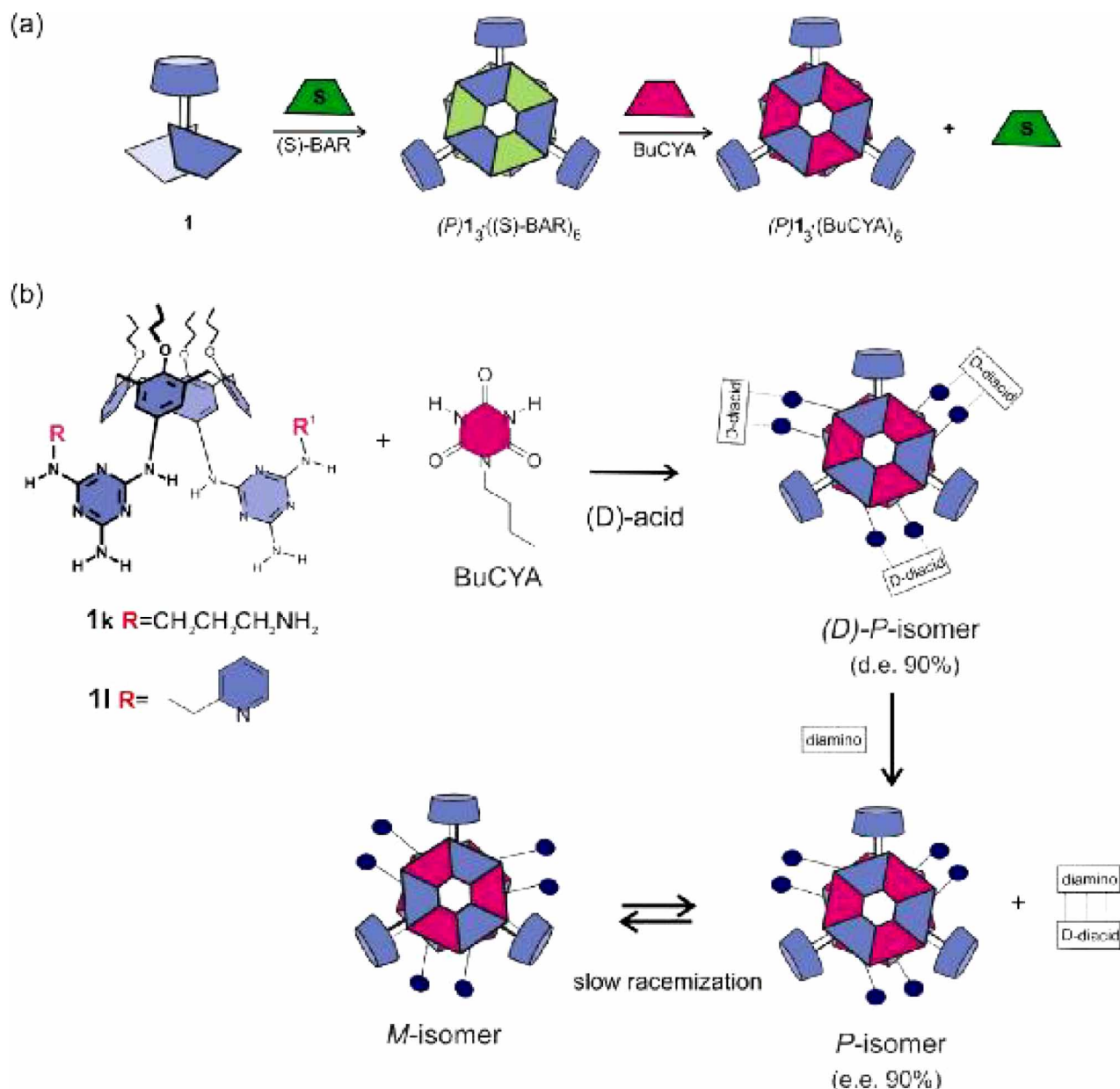
SCHEME 6 Enantioselective noncovalent synthesis of double rosettes exploiting the memory effect. Memory effect (a) by exchanging a chiral barbiturate for an achiral cyanurate and (b) by binding of a chiral guest and its subsequent precipitation.

guest molecule determines the supramolecular chirality of the tetrarosette assembly.

Enantioselective Noncovalent Synthesis

The synthesis of enantiopure self-assembled aggregates based on the "chiral memory" concept implies the use of a chiral auxiliary, used as additive, which interact stereoselectively and in a noncovalent manner with the achiral self-assembled rosette to give preferentially one of the two possible diastereomeric forms of the assembly. When this additive is replaced by an achiral additive, the resulting enantiomer is still optically active although none of its components are chiral [13,41,45,46]. This strategy has been used to synthesize enantiomerically pure

self-assembled double rosette assemblies (Scheme 6) [36]. First, induction of supramolecular chirality was achieved with chiral barbiturates, which are subsequently replaced by achiral cyanurates in a qualitative manner (Scheme 6a). The success of this approach relies primarily on the association between cyanurates and melamines being much stronger than that between barbiturates and melamines, due to the higher acidity of the cyanurates [26,38]. Therefore in these systems, the enantiomerically pure assemblies are obtained from the corresponding diastereomers and not by resolution of the enantiomeric racemic mixture. Following this method an enantiomeric excess (e.e.) of 96% was obtained [36]. On the other hand, the complexation of chiral diacids to amino substituted double rosettes and subsequent removal
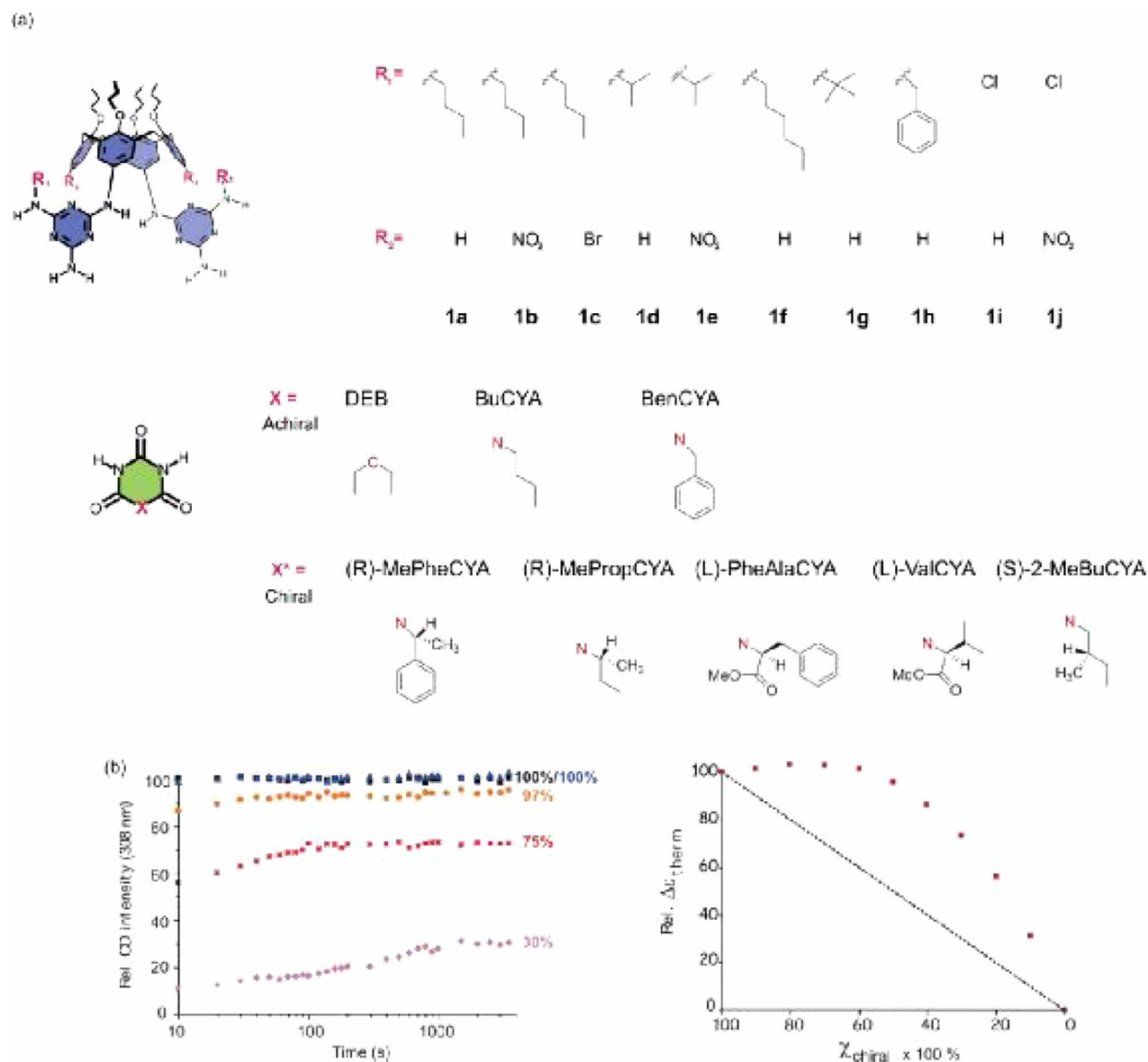
FIGURE 4 (a) Molecular structures of calix[4]arene dimelamines **1a−j** and BAR/CYA derivatives; (b) Left: Plot of the relative CD intensity at 308 nm, versus the time for a mixture of (*P*)-**1b**$_3$·((R)-MePheCYA)$_6$ and **1b**$_3$·(BenCYA)$_6$ with different initial fractions of **1b**$_3$·((R)-MePheCYA)$_6$ (◆: 10%; *: 30%; ●: 50%; ■: 70%; △: 90%) (the percentage of the graphic represents the relative CD-intensity reached at the thermodynamic equilibrium); Right: Plot of the relative CD-intensities at the thermodynamic equilibrium for different mole fractions of chiral component. The dotted line represents the expected CD-intensities when there is no amplification of chirality.

of the acids leads to the generation of the enantiopure assembly. The removal of the diacids is carried out via precipitation of the salt upon addition of amine, obtaining an enantiomeric assembly with an e.e. of 90% (Scheme 6b) [39].

Amplification of Chirality: The "*Sergeant and Soldiers*" Principle

Amplification of chirality is defined as the process in which a high enantiomeric or diastereomeric excess is generated by the presence of small amounts of chiral molecules [47]. The *sergeant and soldiers* principle has been applied to dynamic hydrogen bonded assemblies of well-defined molecular composition (double

rosette assemblies) (Fig. 4) [48]. For example, chiral assemblies ((P)-**1b**$_3$·((*R*)-MePheCYA)$_6$) and racemic assemblies (**1b**$_3$·(BenCYA)$_6$) were mixed in ratios ranging from 1:9 to 9:1 measuring the CD intensity at 308 nm as a function of time at 70°C (Fig. 4). In all the studied cases (Fig. 4) the thermodynamic equilibrium is reached almost immediately after mixing the assemblies. The CD-intensity of the mixtures will follow a linear behavior when there is no amplification of the chirality in the system during the process of increasing the ratio of the chiral assembly present. However, in these studies the typical non-linear behavior of the "*sergeants and soldiers*" principle was observed (Fig. 4). The CD-intensities of the mixtures increase nonlinearly with the percentage of chiral

assembly provided. The ^{1}H-NMR spectrum shows (figure not shown) the presence of several signals in the region of 15–14 ppm due to the generation of heteromeric assemblies ($\mathbf{1b}_3\cdot(\text{BenCYA})_n((R)\text{-}$MePheCYA$)_{6-n}$) ($n = 1$–5). These assemblies lead to the formation of the (P)-diastereomer preferentially.

Moreover, a large variety of systems including chiral and racemic structurally related assemblies have been studied in order to determine which parameters influences the amplification of chirality for these types of hydrogen-bonded assemblies (Fig. 4). The introduction of different substituents in the calix[4]arene dimelamines or cyanurate components of the double rosette assemblies was considered [49]. The introduction of bulky groups in the calix[4]arene dimelamine building blocks (R$_1$, in Fig. 4) decreases the amplification of chirality. In addition, the amplification of chirality is highly influenced by the presence of substituents directly attached to the calix[4]arene skeleton (R$_2$, Fig. 4) obtaining different values depending on the substituents. For example, the influence in the introduction of nitro groups in the calix[4]arene skeleton (**1b**, Fig. 4) leads to systems with a higher degree of chiral amplification. However, the introduction of bromide substituents (**1c**, Fig. 4) induces a decrease in amplification of chirality. These differences can be due to steric or electronic factors introduced by the substituents. On the other hand, the presence of bulky substituents in the cyanurate components leads to an increase in the amplification of chirality.

The amplification of chirality can also be observed for tetrarosette assemblies [50]. The difference in free energy between the two enantiomers (P and M) of the tetrarosettes introduced by a chiral center is higher than for double rosettes because it requires the disruption of 24 hydrogen bonds for the dissociation of one tetramelamine building block. Chiral amplification studies of these assemblies at different molar ratios of chiral component showed the typical nonlinear behavior resulting from the "sergeants and soldiers" principle. It has been observed that the control of amplification of chirality in the rosette systems increases with the number of layers in the assemblies. The high chiral amplification obtained can be compared with the chiral amplification obtained for covalent polymeric structures. Moreover, the flexible spacer between the two layers in the tetrarosette assembly has been substituted for a more rigid phenyl ring resulting in a decreasing in the amplification of chirality, probably due to the introduction of geometric constrains.

Chirality of Rosette Assemblies in 2-D

Highly ordered 2-D arrays of rosette nanostructures can be obtained by deposition of the assemblies from an organic solvent, such as chloroform or toluene, on a freshly cleaved highly oriented pyrolytic graphite (HOPG) surfaces as revealed by AFM studies [51–53].

Deposition of double rosette assemblies showed tightly packed rows with an interrow distance of 3.8 ± 0.2 nm attributed to the face-to-face stacking of the assemblies based on cross-sectional analysis of assemblies with different substituents in the calix[4]-arene unit [54]. In the case of tetrarosette assemblies the interrow spacing obtained of 4.6 ± 0.1 nm is comparable with the double rosettes. These data suggest that the arrangement of the assemblies on the surface is the same as for double rosettes: face-to-face arrangement. The orientations of the rods are related to the underlying substrate, therefore with orientation differences of 60°. However, closer observations and analysis of the domains showed the presence of deviating subdomains (Fig. 5). The orientation of the nanorod domains appears to be $\pm 23°$ with respect to the orientation of the underlying HOPG. These observations are more evident in the case of tetrarosettes due to the formation of higher-order hierarchical structures in 2-D [51]. These orientations were revealed by elucidating the nanometer-scale arrangement of the rosettes by high resolution TM-AFM. As it has been shown in solution the rosette assemblies in absence of elements of chirality they form racemic mixtures of P and M enantiomers. However, after deposition on HOPG surfaces those structures are clearly chiral showing two types of domains with different orientations respect to the nanorod direction. Therefore, spontaneous resolution of the P and M rosettes into enantiopure domains took place on HOPG surfaces after deposition of a racemic mixture [55].

CONCLUSIONS

Here the control over many aspects of the supramolecular chirality of hydrogen-bonded rosette assemblies has been shown resulting in the stereoselective synthesis of diastereomeric and enantiomeric assemblies. Especially, the control over the processes of chiral memory and chiral amplification could have promising applications in the material science field. Furthermore the racemic mixture of self-assembled systems has been spontaneously resolved into enantiopure domains in 2D supramolecular assemblies on HOPG. It is evident that control over supramolecular chirality of synthetic increasingly complex assemblies will be of crucial importance to their application in the field of molecular recognition, catalysis, material sciences, and especially nanotechnology. Nevertheless, issues such as the understanding of the relation between rosette structure and substitution pattern on one
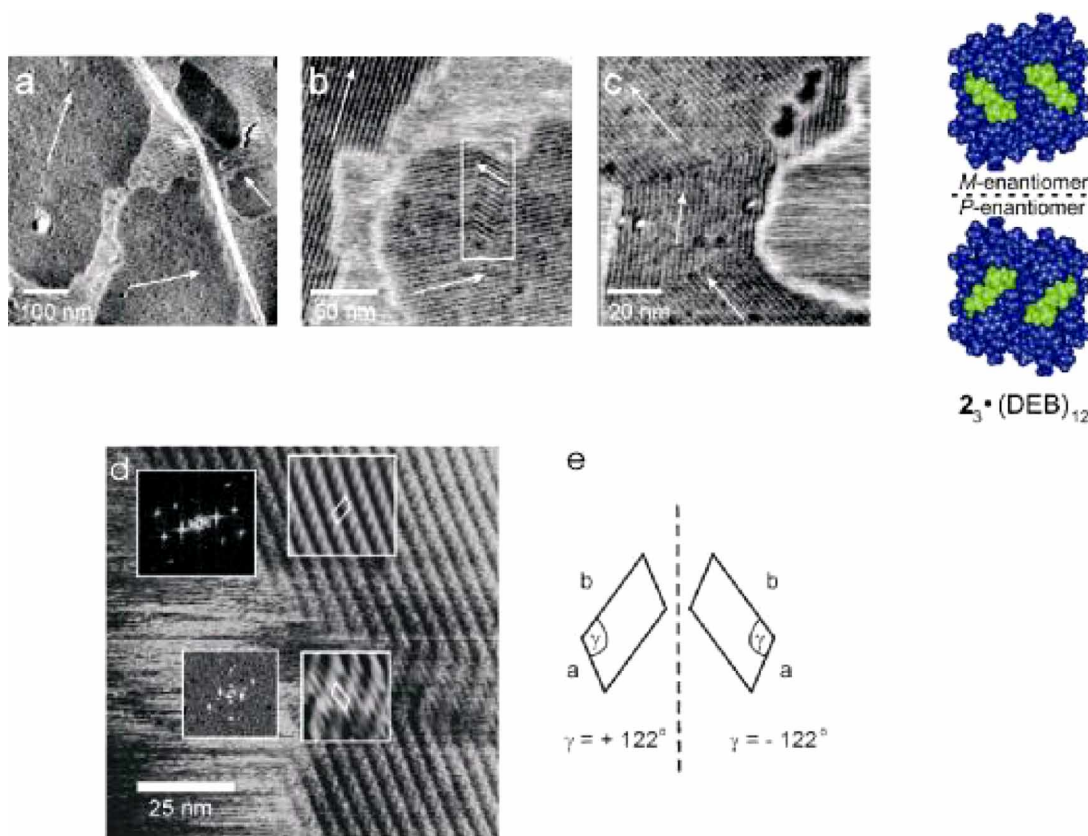
FIGURE 5   TM-AFM phase images of nanorod domains of tetrarosettes $2_3 \cdot (DEB)_{12}$ on HOPG: (a) The orientation of several nanorod domains is related to the threefold symmetry of the HOPG substrate (scan size 600 nm × 600 nm). (b) Within the distinct defect region in the largest domain (inside square) a different orientation with an angle of 46° can be recognized (scan size 200 nm × 200 nm). (c) The angle between different domains on the same sample can be estimated as 46°, as shown by the arrows (scan size 100 nm × 100 nm). (d) TM-AFM phase image of nanorod domains of tetrarosettes $2_3 \cdot (DEB)_{12}$ on HOPG (insets: 2-D FFTs, left; Fourier-filtered sections, right). The unit cell of the structure observed is indicated in the corresponding Fourier-filtered sections. (e) Schematic of the mirror symmetry observed for the two different types of domains shown in Fig. 5d. (From Ref. 53, Copyright 2004 Wiley-VCH, Weinheim).

hand and the orientation of the superstructures on surfaces in 2D on the other hand are challenges that need to be addressed in the future.

References

[1] Lehn, J. -M. *Supramolecular Chemistry, Concepts and Perspectives*; VCH: New York, 1995.

[2] Clines, D. *The Physical Origin of Homochirality in Life*; AIP Press: Woodbury, NY, 1996.

[3] Engelkamp, H.; Middelbeek, S.; Nolte, R. J. M. *Science* **1999**, *284*, 785–788.

[4] Nuckolls, C.; Katz, T. J.; Verbiest, T.; Van Elshocht, S.; Kuball, H. G.; Kiesewalter, S.; Lovinger, A. J.; Persoons, A. *J. Am. Chem. Soc.* **1998**, *120*, 8656–8660.

[5] DeRossi, U.; Dahne, S.; Meskers, S. C. J.; Dekkers, H. *Angew. Chem. Int. Ed.* **1996**, *35*, 760–763.

[6] Ezuhara, T.; Endo, K.; Aoyama, Y. *J. Am. Chem. Soc.* **1999**, *121*, 3279–3283.

[7] Huang, X.; Li, C.; Jiang, S. G.; Wang, X. S.; Zhang, B. W.; Liu, M. H. *J. Am. Chem. Soc.* **2004**, *126*, 1322–1323.

[8] Huang, X.; Liu, M. H. *Chem. Commun.* **2003**, 66–67.

[9] Prins, L. J.; Huskens, J.; de Jong, F.; Timmerman, P.; Reinhoudt, D. N. *Nature* **1999**, *398*, 498–502.

[10] Ribo, J. M.; Crusats, J.; Sagues, F.; Claret, J.; Rubires, R. *Science* **2001**, *292*, 2063–2066.

[11] Viswanathan, R.; Zasadzinski, J. A.; Schwartz, D. K. *Nature* **1994**, *368*, 440–443.

[12] Yang, W. S.; Chai, X. D.; Chi, L. F.; Liu, X. D.; Cao, Y. W.; Lu, R.; Jiang, Y. S.; Tang, X. Y.; Fuchs, H.; Li, T. J. *Chem. Eur. J.* **1999**, *5*, 1144–1149.

[13] Yashima, E.; Maeda, K.; Okamoto, Y. *Nature* **1999**, *399*, 449–451.

[14] Yuan, J.; Liu, M. H. *J. Am. Chem. Soc.* **2003**, *125*, 5051–5056.

[15] Zhai, X. D.; Zhang, L.; Liu, M. H. *J. Phys. Chem. B* **2004**, *108*, 7180–7185.

[16] Zhang, L.; Lu, Q.; Liu, M. H. *J. Phys. Chem. B* **2003**, *107*, 2565–2569.

[17] Zhang, L.; Yuan, J.; Liu, M. H. *J. Phys. Chem.* **2003**, *107*, 12768–12773.

[18] Alberts, B.; Bray, D.; Lewis, J.; Raff, M.; Roberts, K.; Watson, J. D. *Molecular Biology of the Cell*; 2nd ed. Garland: New York, 1989.

[19] Macdonald, J. C.; Whitesides, G. M. *Chem. Rev.* **1994**, *94*, 2383–2420.

[20] Ajayaghosh, A.; George, S. J. *J. Am. Chem. Soc.* **2001**, *123*, 5148–5149.

[21] Ariga, K.; Kunitake, T. *Acc. Chem. Res.* **1998**, *31*, 371–378.

[22] Fernandez-Lopez, S.; Kim, H. S.; Choi, E. C.; Delgado, M.; Granja, J. R.; Khasanov, A.; Kraehenbuehl, K.; Long, G.; Weinberger, D. A.; Wilcoxen, K. M.; Ghadiri, M. R. *Nature* **2001**, *412*, 452–455.

[23] Dapporto, P.; Paoli, P.; Roelens, S. *J. Org. Chem.* **2001**, *66*, 4930–4933.

[24] Jonkheijm, P.; Hoeben, F. J. M.; Kleppinger, R.; van Herrikhuyzen, J.; Schenning, A.; Meijer, E. W. *J. Am. Chem. Soc.* **2003**, *125*, 15941–15949.

[25] Seto, C. T.; Mathias, J. P.; Whitesides, G. M. *J. Am. Chem. Soc.* **1993**, *115*, 1321–1329.

[26] Bielejewska, A. G.; Marjo, C. E.; Prins, L. J.; Timmerman, P.; de Jong, F.; Reinhoudt, D. N. *J. Am. Chem. Soc.* **2001**, *123*, 7518–7533.

[27] Whitesides, G. M.; Simanek, E. E.; Mathias, J. P.; Seto, C. T.; Chin, D. N.; Mammen, M.; Gordon, D. M. *Acc. Chem. Res.* **1995**, *28*, 37–44.

[28] Vreekamp, R. H.; vanDuynhoven, J. P. M.; Hubert, M.; Verboom, W.; Reinhoudt, D. N. *Angew. Chem. Int. Ed.* **1996**, *35*, 1215–1218.

[29] Jolliffe, K. A.; Timmerman, P.; Reinhoudt, D. N. *Angew. Chem. Int. Ed.* **1999**, *38*, 933–937.

[30] Paraschiv, V.; Crego-Calama, M.; Fokkens, R. H.; Padberg, C. J.; Timmerman, P.; Reinhoudt, D. N. *J. Org. Chem.* **2001**, *66*, 8297–8301.

[31] Prins, L. J.; Neuteboom, E. E.; Paraschiv, V.; Crego-Calama, M.; Timmerman, P.; Reinhoudt, D. N. *J. Org. Chem.* **2002**, *67*, 4808–4820.

[32] Timmerman, P.; Vreekamp, R. H.; Hulst, R.; Verboom, W.; Reinhoudt, D. N.; Rissanen, K.; Udachin, K. A.; Ripmeester, J. *Chem. Eur. J.* **1997**, *3*, 1823–1832.

[33] Prins, L. J.; Jolliffe, K. A.; Hulst, R.; Timmerman, P.; Reinhoudt, D. N. *J. Am. Chem. Soc.* **2000**, *122*, 3617–3627.

[34] Timmerman, P.; Jolliffe, K. A.; Calama, M. C.; Weidmann, J. L.; Prins, L. J.; Cardullo, F.; Snellink-Ruel, B. H. M.; Fokkens, R. H.; Nibbering, N. M. M.; Shinkai, S.; Reinhoudt, D. N. *Chem. Eur. J.* **2000**, *6*, 4104–4115.

[35] Timmerman, P.; Prins, L. J. *Eur. J. Org. Chem.* **2001**, 3191–3205.

[36] Prins, L. J.; De Jong, F.; Timmerman, P.; Reinhoudt, D. N. *Nature* **2000**, *408*, 181–184.

[37] Eliel, E. L.; Wilen, S. H. *Stereochemistry of Organic Compounds*; Wiley: New York, 1994.

[38] Prins, L. J.; Hulst, R.; Timmerman, P.; Reinhoudt, D. N. *Chem. Eur. J.* **2002**, *8*, 2288–2301.

[39] Ishi-i, T.; Crego-Calama, M.; Timmerman, P.; Reinhoudt, D. N.; Shinkai, S. *J. Am. Chem. Soc.* **2002**, *124*, 14631–14641.

[40] Ishi-i, T.; Crego-Calama, M.; Timmerman, P.; Reinhoudt, D. N.; Shinkai, S. *Angew. Chem. Int. Ed.* **2002**, *41*, 1924–1929.

[41] Furusho, Y.; Kimura, T.; Mizuno, Y.; Aida, T. *J. Am. Chem. Soc.* **1997**, *119*, 5267–5268.

[42] Ikeda, M.; Takeuchi, M.; Sugasaki, A.; Robertson, A.; Imada, T.; Shinkai, S. *Supramolecular Chem.* **2000**, *12*, 321.

[43] Inai, Y.; Tagawa, K.; Takasu, A.; Hirabayashi, T.; Oshikawa, T.; Yamashita, M. *J. Am. Chem. Soc.* **2000**, *122*, 11731–11732.

[44] Ishi-i, T.; Mateos-Timoneda, M. A.; Timmerman, P.; Crego-Calama, M.; Reinhoudt, D. N.; Shinkai, S. *Angew. Chem. Int. Ed.* **2003**, *42*, 2300–2305.

[45] Kubo, Y.; Ohno, T.; Yamanaka, J.; Tokita, S.; Iida, T.; Ishimaru, Y. *J. Am. Chem. Soc.* **2001**, *123*, 12700–12701.

[46] Sugasaki, A.; Ikeda, M.; Takeuchi, M.; Robertson, A.; Shinkai, S. *J. Chem. Soc. Perkin Trans. 1* **1999**, 3259–3264.

[47] Feringa, B. L.; van Delden, R. A. *Angew. Chem. Int. Ed.* **1999**, *38*, 3419–3438.

[48] Prins, L. J.; Timmerman, P.; Reinhoudt, D. N. *J. Am. Chem. Soc.* **2001**, *123*, 10153–10163.

[49] Mateos-Timoneda, M. A.; Crego-Calama, M.; Reinhoudt, D. N. *Supramolecular Chem.* **2005**, *17*, 67–79.

[50] Mateos-Timoneda, M. A.; Crego-Calama, M.; Reinhoudt, D. N. *Chem. Eur. J.* **2006**, *12*, 2630–2638.

[51] Schonherr, H.; Paraschiv, V.; Zapotoczny, S.; Crego-Calama, M.; Timmerman, P.; Frank, C. W.; Vancso, G. J.; Reinhoudt, D. N. *PNAS* **2002**, *99*, 5024–5027.

[52] van Manen, H. J.; Paraschiv, V.; Garcia-Lopez, J. J.; Schonherr, H.; Zapotoczny, S.; Vancso, G. J.; Crego-Calama, M.; Reinhoudt, D. N. *Nano Lett.* **2004**, *4*, 441–446.

[53] Schonherr, H.; Crego-Calama, M.; Vancso, G. J.; Reinhoudt, D. N. *Adv. Mater.* **2004**, *16*, 1416–1420.

[54] Klok, H. A.; Jolliffe, K. A.; Schauer, C. L.; Prins, L. J.; Spatz, J. P.; Moller, M.; Timmerman, P.; Reinhoudt, D. N. *J. Am. Chem. Soc.* **1999**, *121*, 7154–7155.

[55] Schonherr, H.; Calama, M. C.; Vansco, J. G.; Reinhoudt, D. N. *Dekker Encyclopedia of Nanoscience and Nanotechnology*; Marcel Dekker, Inc. New York, 2004; pp 155–167.